Translational Stroke Research
https://doi.org/10.1007/s12975-020-00843-8

REVIEW ARTICLE

A Review of Translational Magnetic Resonance Imaging in Human and Rodent Experimental Models of Small Vessel Disease

Michael S. Stringer[1,2] · Hedok Lee[3] · Mikko T. Huuskonen[4,5] · Bradley J. MacIntosh[6,7,8] · Rosalind Brown[1,2] · Axel Montagne[4,5] · Sarah Atwi[6,7] · Joel Ramirez[6,8] · Maurits A. Jansen[9] · Ian Marshall[1,2] · Sandra E. Black[6,8,10] · Berislav V. Zlokovic[4,5] · Helene Benveniste[3] · Joanna M. Wardlaw[1,2]

Received: 1 June 2020 / Revised: 16 August 2020 / Accepted: 19 August 2020

Abstract

Cerebral small vessel disease (SVD) is a major health burden, yet the pathophysiology remains poorly understood with no effective treatment. Since much of SVD develops silently and insidiously, non-invasive neuroimaging such as MRI is fundamental to detecting and understanding SVD in humans. Several relevant SVD rodent models are established for which MRI can monitor in vivo changes over time prior to histological examination. Here, we critically review the MRI methods pertaining to salient rodent models and evaluate synergies with human SVD MRI methods. We found few relevant publications, but argue there is considerable scope for greater use of MRI in rodent models, and opportunities for harmonisation of the rodent-human methods to increase the translational potential of models to understand SVD in humans. We summarise current MR techniques used in SVD research, provide recommendations and examples and highlight practicalities for use of MRI SVD imaging protocols in pre-selected, relevant rodent models.

Keywords Small vessel disease · Magnetic resonance imaging · Systematic reviews · Lacunar infarcts · Dementia · Brain imaging

Michael S. Stringer, Hedok Lee, Mikko T. Huuskonen and Bradley J. MacIntosh are joint first authors.

Sandra E. Black, Berislav V. Zlokovic, Helene Benveniste and Joanna M. Wardlaw are joint last authors.

Electronic supplementary material The online version of this article (https://doi.org/10.1007/s12975-020-00843-8) contains supplementary material, which is available to authorised users.

✉ Joanna M. Wardlaw
joanna.wardlaw@ed.ac.uk

[1] Brain Research Imaging Centre, Centre for Clinical Brain Sciences, University of Edinburgh, Edinburgh, UK

[2] UK Dementia Research Institute, Edinburgh Medical School, University of Edinburgh, Edinburgh, UK

[3] Department of Anesthesiology, Yale School of Medicine, Yale University, New Haven, CT, USA

[4] Zilkha Neurogenetic Institute, Keck School of Medicine, University of Southern California, Los Angeles, CA, USA

[5] Department of Physiology and Neuroscience, Keck School of Medicine, University of Southern California, Los Angeles, CA, USA

[6] Heart and Stroke Foundation Canadian Partnership for Stroke Recovery, Sunnybrook Research Institute, University of Toronto, Toronto, ON, Canada

[7] Department of Medical Biophysics, University of Toronto, Toronto, ON, Canada

[8] Hurvitz Brain Sciences Research Program, Sunnybrook Research Institute, Toronto, ON, Canada

[9] Edinburgh Preclinical Imaging, Centre for Cardiovascular Science, University of Edinburgh, Edinburgh, UK

[10] Department of Medicine (Neurology), University of Toronto, Toronto, ON, Canada

Published online: 16 September 2020

Introduction

Cerebral small vessel disease (SVD) is estimated to cause 20–25% of strokes globally and 45–65% of dementias [1, 2]. Magnetic resonance imaging (MRI) is used extensively in clinics and research to identify SVD-associated lesions and imaging biomarkers. Key SVD-related features, image acquisition and quantification methods are summarised in recent position papers [3, 4].

The core diagnostic SVD protocol includes the following: T1-weighted (T1-w), to provide detailed anatomical images, identify brain atrophy and differentiate grey/white matter; T2-weighted (T2-w), to distinguish lacunes from dilated perivascular spaces (PVS) or white matter hyperintensities (WMH); fluid-attenuated inversion recovery (FLAIR), to identify WMH, lacunes and established infarcts; diffusion-weighted imaging (DWI), to detect recent small infarcts due to high sensitivity to acute ischaemia [5]; and blood sensitive (gradient echo (GRE)/T2*-w or susceptibility-weighted imaging), to identify cerebral microbleeds, superficial siderosis and mineral deposition [3].

Advanced MRI techniques aid research into SVD pathogenesis [6] including DTI, to assess white matter integrity, and methods, to assess microvascular function, including cerebrovascular reactivity (CVR), intracranial vascular and cerebrospinal fluid (CSF) pulsatility, cerebral blood flow (CBF) and blood–brain barrier (BBB) integrity. Dynamic and static CBF is important in assessing cerebrovascular health [7]. Dynamic blood flow responsiveness is commonly assessed with blood oxygenation level–dependent (BOLD) [8]. Resting CBF can be measured by dynamic susceptibility contrast (DSC), arterial spin labelling (ASL) and phase contrast MRI (PC-MRI). Dynamic contrast-enhanced (DCE) MRI using intravenous injection of gadolinium (Gd) contrast [9] shows increased BBB permeability in SVD [4, 10–12]. Magnetic resonance spectroscopy (MRS) detects neuro-metabolite changes, including evidence of axonal loss/disruption [13, 14].

Various rodent models reflect different putative SVD mechanisms and some features of human disease [15–19]. Hypertension models replicate elements of microvessel remodelling from some sporadic human SVD [20], including venous collagenosis [21], but hypertension is only one risk factor. The spontaneously hypertensive stroke prone rat (SHRSP) has endothelial dysfunction, microglial, white matter and BBB abnormalities prior to hypertension and sporadic SVD features when older [18]. Bilateral carotid artery microcoils to induce mild stenosis (BCAS) leads to some SVD characteristics [22, 23] but may work through altering carotid elasticity and arterial pulsatility. There are also several monogenic SVD and knockout models [19, 24, 25].

There are some inherent limitations to the translational potential of animal models [15, 16, 18]. Anatomically, white:grey matter ratios and brain sizes differ markedly (Fig. 1) [15, 16]; arterial anatomy [26, 27], density, spacing and positioning of penetrating arterioles and draining venules also vary [28]. In stroke models, assessing rodent neurological deficits is challenging when symptoms are mild and recovery may be rapid [29]. Anaesthetics, necessary for many types of study, can affect cerebral haemodynamics and CSF transport [30] and may provide neuroprotective or adversive effects that could alter the tissue changes [31, 32]. Rodent respiratory and heart rates are higher, restricting options for physiological measurements and pulse gating required for some MR sequences at comparable temporal resolution to humans.

Despite the anatomical and physiological differences from humans, rodent SVD models are however key for investigating pathological processes and time trajectories of disease evolution and developing and testing novel therapies [33]. Preclinical MRI facilitates independent validation with contemporaneous histology or other imaging techniques and improves clinical translation and exploration of physiological processes, e.g. fluid flow through the glymphatic system [34–36], glymphatic system changes during sleep [37] and effects of risk factors, including hypertension and diabetes, on tissue damage and microvascular fluid dynamics [38, 39].

As part of efforts to improve the translational value of preclinical models to human SVD, particularly through the use of MRI, we reviewed the literature to identify studies which had adapted clinical MRI methods to preclinical MRI, or vice versa. Our intention is not to review preclinical SVD rodent models but rather to evaluate synergies, strengths and limitations between human and rodent MRI to optimise the translational potential of MRI for non-invasive longitudinal assessment of disease development and progression in SVD.

Methods

Systematic Review

We reviewed the literature to extract information on approaches to improving comparability or complementarity of brain MRI techniques between studies in rodents and humans. The systematic literature search was conducted on Medline and Embase from 1946 until April 2020 through Ovid. Exploded headings and search terms relating to SVD were combined with terms for MRI and relevant advanced MR

techniques. We also combined these results with a comprehensive search strategy for rodents based on Hooijmans et al.'s filter [40] and terms associated with translational research (e.g. translat*, retranslat*) prior to limiting to papers relating to humans. Finally, we removed duplicates. For the full search strategy, see the Supplementary Material.

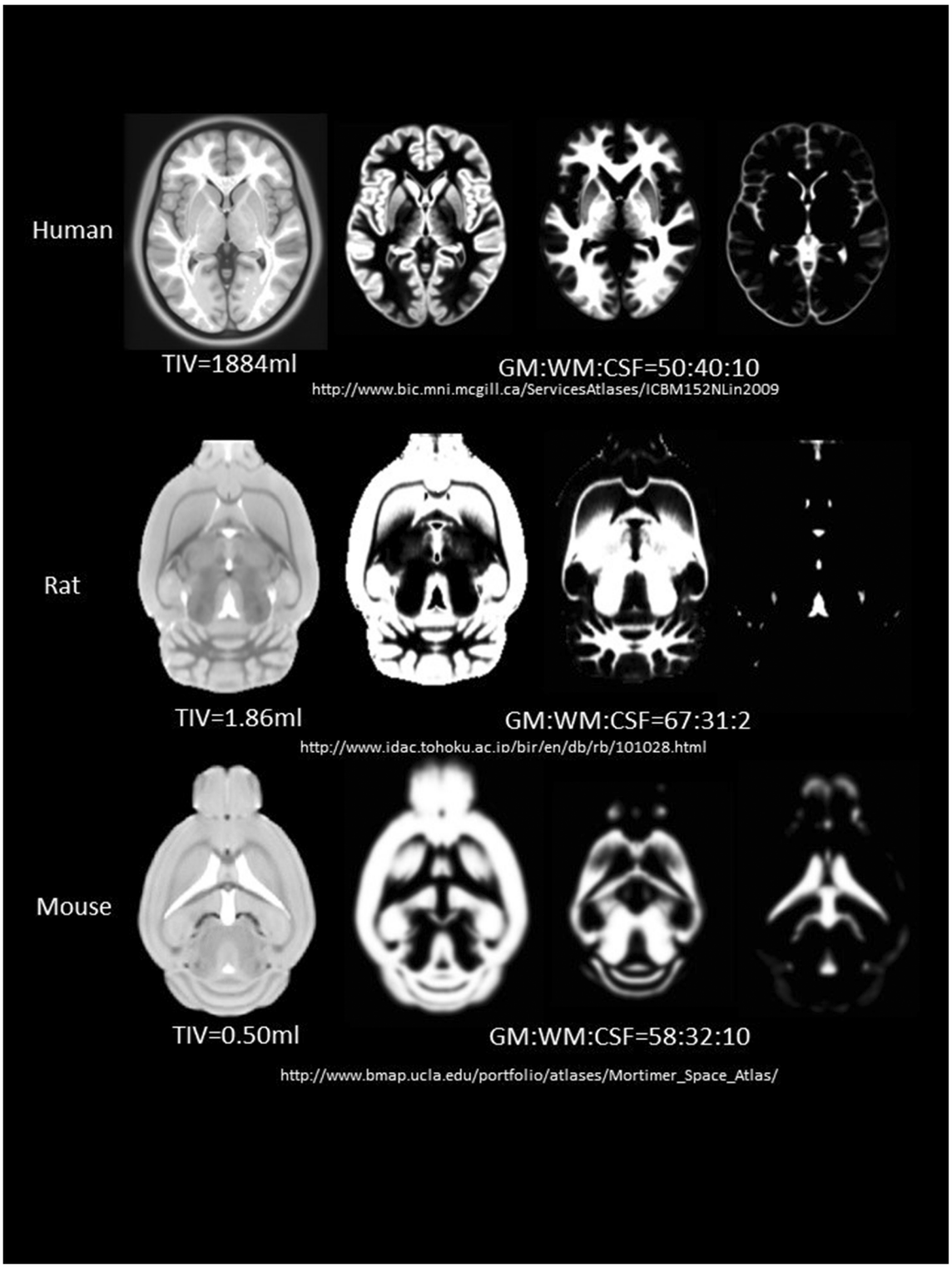

Fig. 1 Approximate total intracranial volume (TIV) volume (ml) and grey matter:white matter:CSF ratio in healthy (young) animals shown relative to the human brain based on publicly available templates

We also manually checked reference lists in reviews and original papers for additional relevant references. Other papers were identified from the authors' libraries. We inspected all identified papers to ascertain whether they satisfied the eligibility criteria. We included papers that provided information on MRI methods designed to be used in humans and those designed for use in rodent models but that aimed to capture SVD features, including static [41] and dynamic biomarkers (e.g. vascular reactivity and BBB dynamics), which use similar sequences in rodents and humans including practical guidance. We excluded studies published solely as conference abstracts due to providing insufficient detail.

One author (MSS) extracted summary data for each paper including the type of publication, diseases covered, imaging techniques employed and a short summary of the focus. Other authors resolved uncertainties. We sought to provide an overview of all published strategies for comparable human-rodent MR imaging protocols, practicalities and advice on specific sequence(s) including structural, post-mortem and dynamic vascular function assessments including CVR and DCE.

Results

The search identified 305 unique publications of which we excluded 260 as irrelevant based on the title, mainly due to being in an unrelated population, case reports or modality (e.g. positron emission tomography (PET), computed tomography (CT)) (Fig. 2). On full-text review of the remaining 45, a further 30 were excluded, mainly due to the following: no MRI (12), translation of other biomarkers for drug development (five), clinical or preclinical studies only (six), conference abstracts (six) and one book.

Of the 15 relevant papers that addressed any aspect of rodent-human MRI, seven were narrative reviews [42–48], one was an editorial [49] and seven were original research [22, 50–55] (Table 1). Of these, six focused on AD (four reviews [42–45], one editorial [49] and one original paper [52]), one review [47] on stroke, two original papers on Huntington's disease [51, 54], one original paper each on ageing [50] and hypertension [55], two original papers [22, 53] and one review on SVD [48] and one review briefly summarised functional MRI (fMRI) applications in several diseases [46], including stroke and neurodegeneration.

All studies were cross-sectional [22, 50, 52–55] with the exception of the preclinical component of [51] which was longitudinal.

We found no protocol with guidance on designing longitudinal MRI studies in rodents to mirror typical MRI research to examine disease development in human cohorts. One rodent protocol used DTI, T2w, T1w and T2*w but not FLAIR [22]. No studies addressed image analysis issues that are commonly encountered in human studies, such as image registration and lesion tracking over time, or combining data from several different sequences from the same anatomical regions or lesions at one time point. We did find a few studies where assessment tools developed to assess SVD features in humans, such as the Fazekas scale for WMH [56], Brain Observer MicroBleed Scale (BOMBS) for cerebral microbleeds [57] and several image analysis methods such as segmentation and voxel-based morphometry, have been adapted for use in animal models [22, 54]. We also found one example of a novel imaging approach developed to assess perivascular space fluid uptake in rodents that had been translated to human use [53].

There were few studies where MRI had been used to assess response to treatment in rodents [42, 43]. The review papers highlighted several complementary methods including microscopy [45] and functional [43, 45, 46] and in vivo and ex vivo structural MR imaging [22, 42, 44, 45, 50] (Table 1). However, these methods were only rarely used

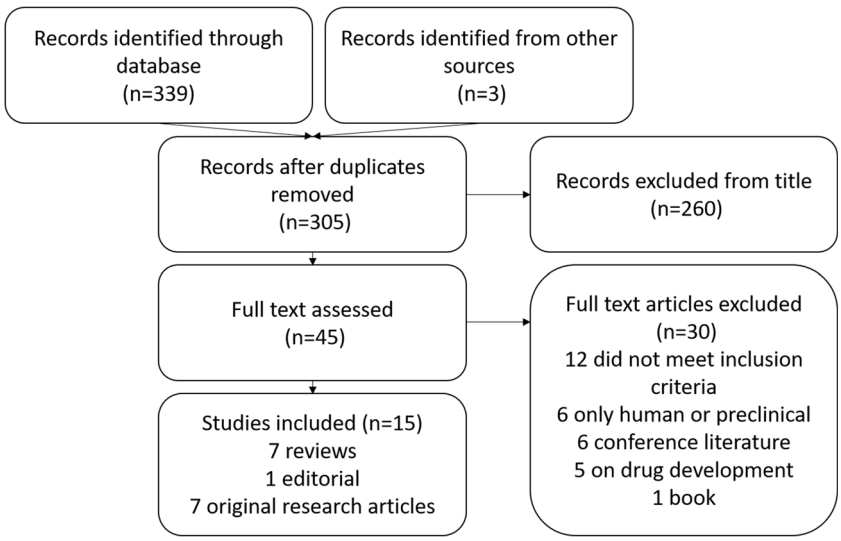

Fig. 2 PRISMA flow diagram of the literature search

Table 1 Summary of studies included in the literature review

Authors	Type	Disease	Methods	Focus
Beckmann (2011) [43]	Review	AD	Dynamic susceptibility contrast, arterial spin labelling, MR angiography (MRA) and wall shear stress	Different approaches to measuring cerebrovascular changes in humans and transgenic mice
Braakman et al. (2009) [44]	Review	AD	Structural MRI	Reviews the challenges of imaging amyloid plaques in vivo in mice with MR, building on initial work with ex vivo human brain tissue [58], and summarises the outstanding technical barriers to translating such methods to humans
Delatour et al. (2010) [45]	Review	AD	Structural MRI, diffusion MR, MRA, cerebral blood volume, MRS, PET, microscopy techniques	Overview of imaging biomarkers in AD mouse models and their potential for translation with some consideration of the technical barriers.
Kincses et al. (2015) [42]	Review	AD	Structural MRI (voxel-based morphometry and diffusion-weighted) and molecular imaging	Primarily structural biomarkers including features where findings in human and animal models overlap, challenges of finding animal models mirroring imaging characteristics of the disease in humans
Keene et al. (2016) [49]	Editorial	AD	Structural and functional MRI/PET, CSF and cognitive assessment	Standardised approach to characterising mouse models based on neuropathological features incorporated in guidelines from the National Institute on Aging and Alzheimer's Association
Meadowcroft et al. (2009) [52]	Original research	AD	Structural MR, histology and electron microscopy	Post-mortem MR, electron microscopy and histology of beta-amyloid plaques in humans with AD and *APP/PS1* transgenic mice to reveal the interplay between the plaques and relaxation mechanisms
Pan et al. (2015) [46]	Review	Stroke, epilepsy, neurodegenerative disease, stress and depression	BOLD MRI	Challenges of translating resting state functional MRI paradigms from humans to rodent models. Limited summary of applications in several different conditions.
Muir et al. (2016) [47]	Review	Stroke	MR/CT angiography and perfusion	Application of imaging as a part of trial recruitment and a study endpoint which can lead to more efficient study design while providing non-invasive measures at an earlier stage
Chaumeil et al. (2012) [51]	Original research	Huntington's	MR spectroscopy	Rodent-human ^{31}P MRS protocol which provides some guidance on the different considerations involved in the two aspects of the study
Sawiak et al. (2013) [54]	Original research	Huntington's	Structural MRI	Development of voxel-based morphometry for mouse models assessed in a Huntington's model
Holland et al. (2011) [50]	Original research	Ageing	Structural MRI, DTI and magnetisation transfer (MT)	Translation of DTI and MT protocols to a bilateral common carotid stenosis mouse model of ageing.
Holland et al. (2015) [22]	Original research	SVD	Structural MRI, DTI and histology	Application of radiological assessment and DTI in a bilateral common carotid stenosis mouse model to explore gliovascular alterations
Wardlaw et al. (2020) [48]	Review	SVD	Structural MRI, DCE-MRI phase contrast, and advanced dynamic MRI scans	Review of current knowledge and outstanding questions on PVS function with a focus on the scope for translation

Table 1 (continued)

Authors	Type	Disease	Methods	Focus
Li et al. (2015) [55]	Original research	Hypertension	Structural MRI, ASL and magnetic resonance angiography	Application of multimodal MRI to assess vessel diameter of cerebral and downstream arteries in relation to the effects on CBF and vascular reactivity
Wang et al. (2020) [53]	Original research	Small vessel diseases	Structural MRI (susceptibility-weighted imaging, SWI)	Use of ultra-small super-paramagnetic iron oxide contrast agents for imaging of small vessels in rodents and humans, with a preclinical histological validation

together in the same study for validation [49]. Lastly, several technology [44] or transferability [45, 46] limitations for clinical to preclinical and vice versa were highlighted, including the need for further validation and methodological advancements to provide scans with higher sensitivity and specificity. There was no detailed overview of a range of MR imaging techniques applied in rodents in disease- or lesion-specific contexts to mirror those developed to study human SVD [3].

Proposed Approaches to Improve the Potential of Rodent-Human Translational MRI

Structural MRI in Rodents and Humans

Human SVD features are present in many models [15, 17, 18, 50]. Certain features are less commonly reported; however, PVS were only recently identified clinically and appear on histology in pericyte-deficient mice [19]. Therefore, optimised parameters enhancing visibility of disease-related features should be used and standardised where possible (https://harness-neuroimaging.org/) [4].

Translational SVD research must account for practical differences. Rodent imaging needs ultra-high magnetic field strengths (i.e. ≥ 7 T) as a necessary and common means of increasing signal-to-noise ratio due to smaller spatial resolution. In human imaging, acquisitions can be accelerated via several techniques, including compressed sensing and parallel imaging [59, 60], thereby reducing motion artefact while allowing incredibly detailed 3D acquisitions in clinically acceptable times; however, such acceleration methods are often less readily available on preclinical platforms. Variations in preclinical pulse sequences may affect comparability of contrast-to-noise ratio (CNR) and image interpretation (Fig. 3). Applying clinical imaging protocols may better integrate translational work, track disease progression/assessment (Fig. 4) and improve cross-model methodological translatability.

Possible exemplar sequences, based on ones found to be reliable and informative at the authors' sites, are listed in Table 2. Options include 2D or 3D sequences, but while 3D are desirable, they take longer than 2D, so 2D may be preferable in some situations.

Validation of pathogenic mechanisms, tissue changes and evolution, complemented by invasive measurements, e.g. 2-photon [38] and post-mortem microscopy, are main reasons for using preclinical models. Preclinical imaging allows longer/more regular scanning and examination using multiple modalities. Advanced structural scans provide useful additional metrics, e.g. DTI for white matter tract integrity/visualisation, and network connectivity assessment, which may help explore cognitive/functional deficits.

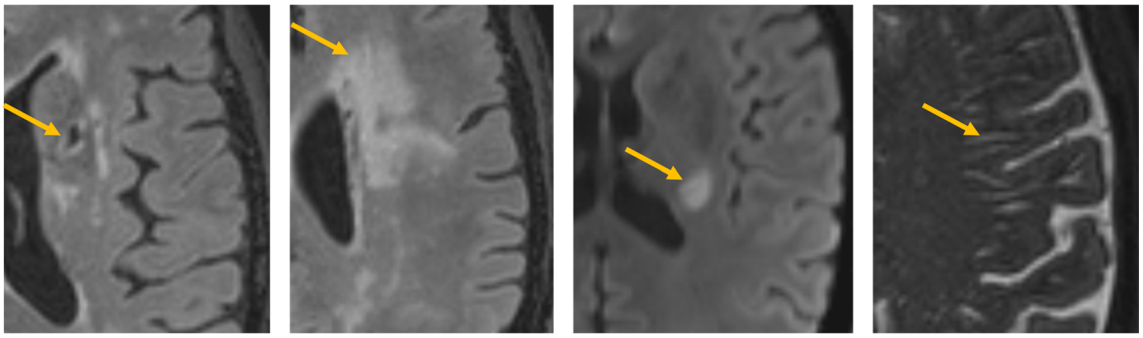

Fig. 3 Examples of the appearance of SVD features in human, from left to right: recent small subcortical (i.e. acute lacunar) infarct (DWI), WMH (FLAIR), lacune (FLAIR) and enlarged perivascular spaces (T2-w) indicated by yellow arrows

Anatomical factors that may affect the translational potential include appropriate metrics/methods to control for relative brain size/tissue ratios and the effects of interventions to increase SVD burden. Clinical SVD features typically increase with age; hence, while using naturally aged rodents [61] may be more challenging and costly, they may reveal more obvious features plus be relevant to longitudinal studies and valuable for preclinical drug testing.

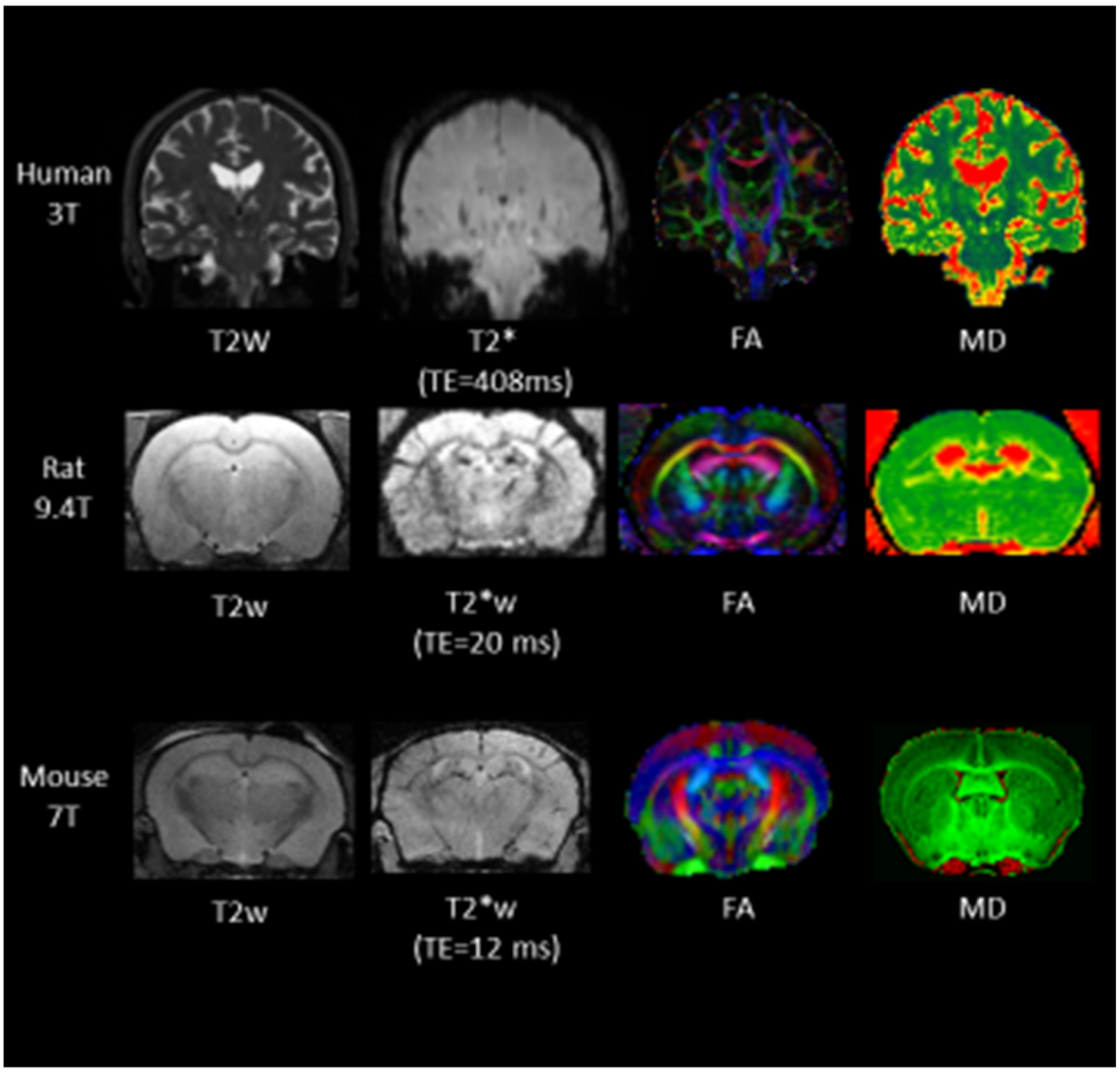

Fig. 4 Illustrations of commonly used structural imaging contrasts in human, rat and mouse models (Human 3 T: MS/JMW, Rat: HL, Mouse: AM). 7 T, 9.4 T and even higher field strengths are commonly used in rodent imaging

Table 2 Exemplar image acquisition parameters for a standard clinical neurovascular structural protocol and possible rodent counterparts at co-authors' sites

Sequences	Purpose	Typical clinical parameters (3 T)	Typical preclinical parameters for rats (7 and 9.4 T)	Typical preclinical parameters for mice (7 and 9.4 T)
T1w	Detailed anatomy	3D, voxel size: 1 mm isotropic, TR/TE = 2500/4.37 ms, TI = 1100 ms, ~ 4 min	2D, voxel size: 0.20 × 0.20 × 0.8 mm, TR/TE 780/9.5 ms, ~ 5 min	2D, voxel size: 0.07 × 0.07 × 0.4 mm, TR/TE = 700/11 ms, ~ 10 min
T2w	Lacunes, PVS	3D, voxel size: 0.9 mm isotropic, TR/TE = 3200/408 ms, ~ 4 min	2D, voxel size: 0.1 × 0.07 × 0.3 mm, TR/TE = 4000/26 ms, ~ 9 min	2D, voxel size: 0.07 × 0.07 × 0.4 mm, TR/TE = 5000/45 ms, ~ 9 min
FLAIR	WMH, juxtacortical or ventricular lesions	3D, voxel size: 1 mm isotropic, TR/TE = 5000/388 ms TI = 1800 ms, ~ 6 min	2D, voxel size: 0.34 × 0.34 × 1.0 mm, TR/TE 8000/30 ms, TI 1930 ms, ~ 10 min	2D, voxel size: 0.13 × 0.13 × 0.5 mm, TR/TE = 6000/15 ms, TI = 1700 ms, ~ 12 min
T2*w/GRE or SWI	Microbleeds, prior ICH, cortical siderosis, tissue mineral deposition; separate intracranial contents from skull	2D, voxel size: 0.6 × 0.6 × 3 mm, TR/TE = 28/20 ms, flip angle = 9°, ~ 4 min (SWI)	3D, voxel size: 0.08 × 0.08 × 0.03 mm, TR/TE = 32/15 ms, flip angle = 12°, ~ 10 min (GRE)	2D, voxel size: 0.06 × 0.06 × 0.5 mm, TR/TE = 415/5 ms, flip angle = 12°, ~ 10 min (GRE)
DWI/DTI	Acute ischaemic lesions; fractional anisotropy (FA), mean diffusivity, tract integrity, tractography	2D, voxel size: 1.3 × 1.3 × 3 mm, TR/TE = 4000/75 ms, 30 directions, ~ 6 min	2D, voxel size: 0.17 × 0.17 × 0.7 mm, TR/TE = 5000/20 ms, 30 directions, ~ 20 min	2D, voxel size: 0.15 × 0.23 × 0.5 mm TR/TE = 3000/32 ms, 30 directions, ~ 10 min
PD	Separate intracranial contents from skull to measure ICV; a few centres use for lesion differentiation (not used in STRIVE)	3D, voxel size: 1 × 1 × 1 mm, TR/TE = 6.04/2.44 ms, ~ 2 min	2D, voxel size: 0.1 × 0.07 × 0.3 mm, TR/TE = 4000/4 ms, ~ 9 min	2D, voxel size: 0.07 × 0.07 × 0.4 mm, TR/TE = 5000/8 ms, ~ 9 min

Times refer to total sequence acquisition time. *TR* repetition time, *TE* echo time, *TI* inversion time

A Greater Role for Post-Mortem MRI in Humans and Rodents

Post-mortem MR (PM-MRI) shows the neuropathology and macroscopic tissue damage underlying MRI features [62, 63]. Long scans are much more feasible PM yielding better image quality with corresponding benefits to signal-to-noise ratio (SNR), spatial resolution and reduced partial volume, thereby enabling precise MR-histology comparisons. Formalin-perfusion fixation improves contrast-to-noise (CNR) for MR microscopy; while SVD lesions remain conspicuous [51, 64–66], prolonged fixation may also induce signal artefacts obscuring lesions [67] and discriminating between pre- and post-mortem damage on MRI may be more challenging (e.g. small parenchymal haemorrhage versus post-mortem intravascular thrombus) [68]. While perfusion fixation is the gold standard for preclinical models, immersion is often preferred in humans for practical reasons. Optimal perfusion fixation is also important to avoid post-mortem intravascular thrombus mimicking pre-mortem intravascular thrombus for example [69]. The time of sacrifice and fixation method must therefore be carefully considered. There are validated protocols relating pre-mortem and PM human MR-visible SVD lesions to histology [62, 70, 71]. While some features may be less evident at PM, PM-MRI is well-suited to automated analysis and is underused in SVD research.

Few papers directly compare PM-MRI to histology [72–75]. Non-quantitative analyses, assessing overall distribution and size [76], risk missing heterogeneous WMH features, including pathological variation [77]. There are limited data on lesion development in rodents during normal ageing; optimisation studies could explore histological-MRI correlates across the lifespan. Close scrutiny of structural and quantitative images by experts in human MRI may identify lesion development stages on PM-MRI. Ex vivo DTI gives data for large areas of tissue and thus can complement and guide the 'spot sampling' approaches typical of histological assessment of white matter integrity [78, 79].

Cerebral microinfarcts (CMIs), small ischaemic lesions encompassing neuronal loss, gliosis and cavitation [80], can appear acutely on diffusion imaging. However, size and signal transience may lead to underestimation of frequency and involvement [71, 81]. PM-MRI allows direct histopathological validation of specific imaging markers [82] including in rodent models. Studies comparing ex vivo MR with histology of CMIs are sparse. More studies would help determine the role of CMIs in SVD and neurodegeneration and help improve the spatial resolution.

Cerebral microbleeds (CMBs), small chronic haemorrhages, appear hypointense on T2*-w/SWI [3, 83] and are not visible on other sequences. CMBs remain visible post-mortem, mirroring histopathology and pre-mortem appearances [84, 85]. Underlying pathological features occurring within CMBs include acute/old (macro)haemorrhages and residual haemosiderin [86]. Paramagnetic properties cause blooming, lesion size overestimation and potential false positives on MRI [87], reinforcing the value of targeted histology alongside MRI measurements. Haemosiderin deposition is detected [19, 88] in amyloid pathology mice, in whom T2*-w CMBs are also reported to correlate with histology [89, 90]. Susceptibility-weighted or quantitative susceptibility imaging may improve sensitivity and accuracy for CMBs, separating haemorrhage from mineralisation, but confirmatory neuropathological studies are warranted [91, 92].

Advanced Dynamic MRI Methods In Vivo in Rodents and Humans

Cerebral Blood Flow and Cerebrovascular Reactivity

CVR refers to vasodilation and vasoconstriction of cerebral microvessels, typically to vasoactive stimuli (e.g. increased CO_2 inspiration or intravenous acetazolamide). CVR is a quintessential cerebrovascular health measure that reflects the role of blood vessels in regulating CBF, oxygen and nutrient delivery, waste product clearance and dissipating heat [93]. CBF is generally measured at rest, with ASL being a widely used method [94].

Several studies have imaged CBF and CVR in SHR and Wistar Kyoto (WKY) rats [55, 95]. However, anaesthetic agents can affect resting CBF and haemodynamic responses and therefore are particularly important to consider when planning experiments on CBF or CVR. For example, CBF was higher in SHR versus in WKY under 2% isoflurane but not with alpha-chloralose and isoflurane reduced CVR [96]. As in preclinical functional neuroimaging, sedation rather than full anaesthesia is often preferred [46]. Dexmedetomidine depresses global CBF; therefore, in some experiments, general anaesthesia with inhalational agents may be preferable. Anaesthetic protocols should also minimise impact on signal and derived imaging variables; further optimisation studies and standardised reporting of anaesthetic protocols would be beneficial.

CVR requires a physiological manipulation/challenge but voluntary breath holding is unsuited to preclinical studies [97] and controlled hypercapnia via breathing apparatus is more reliable. In rats and larger murine models, intubation provides greatest control of inhaled and exhaled gases and is optimal for preclinical CVR. Sealed chambers are practical where intubation is unviable or lower level sedation is preferred. Since CO_2 tolerance varies between species [98, 99], tolerability should be balanced against inducing robust signal changes. Humans tolerate a 6% CO_2 stimulus well [99].

CVR analyses typically use regression models but must account for physiological and practical factors, notably

haemodynamic delays, and filtering band frequency may vary under anaesthesia [46].

CVR has not been fully exploited in rodents to better understand how impaired vasoreactivity develops at whole brain level and leads to brain damage in SVD. Longitudinal CVR measurements coupled with multiphoton microscopy via cranial windows or isolated vessel preparations [100] could strengthen the direct validation of in vivo CVR and improve its use as a biomarker and an intermediary outcome in trials of therapeutic interventions.

Blood–Brain Barrier Impairment

The BBB plays a central role in brain homeostasis, controlling exchange of fluids and selected molecules while protecting parenchyma from potentially toxic plasma components [101]. BBB breakdown occurs in neurodegenerative diseases, including Alzheimer's, Huntington's and SVD [102–107].

MRI, contrast-enhanced CT (CE-CT), PET and biofluid biomarker approaches can measure BBB permeability [4]. MRI methods include dynamic or static contrast-enhanced MRI [4, 11] and non-contrast-based methods (e.g. ASL [108, 109] and T1-w black-blood imaging [110]). The most widely used method to detect subtle focal BBB permeability increases is DCE-MRI [102]. Preclinical validation is limited, but in vivo BBB measures would complement histologic assessment and validation of BBB dysfunction.

DCE-MRI involves T1-mapping followed by intravenous Gd injection and repeated T1-w sequences [111]. Multi-slice or volume sequences, usually GRE or fast low-angle shot, run repeatedly for ca. 20 min; longer acquisitions may be appropriate for low-level leakage [112, 113]. Sequence optimisation balances coverage, SNR and spatial and temporal resolution. As pharmacokinetic analysis requires reliable arterial or venous input functions, identifiable vessels must be covered, e.g. internal carotid arteries or sagittal sinus. High temporal resolution is critical for bolus injections due to rapid blood signal changes [113, 114]. A dilute contrast phantom adjacent to the animal's head can allow signal-to-concentration transformation correction. Anaesthesia level, temperature and respiration should be monitored and adjusted to minimise input function variation.

BBB function parameters, such as volume transfer constants between extracellular space and plasma, are derived by modelling the Gd concentration-time curve, along with CBF and cerebral blood volume. There is now dedicated software for clinical and preclinical DCE analyses (e.g. *ROCKETSHIP* [115]). Patlak models are best suited to subtle BBB leakage in SVD [112, 113]. Retinal imaging, MR venography [116] and phase contrast MRI [117] have been used as surrogates to direct measurement of vessel diameter in response to stimuli; further studies, particularly in humans at field strengths ≥ 7 T, may provide more detailed insight into properties of the microvasculature. Preclinically, methods like multiphoton microscopy can also complement DCE-MRI by determining the microvascular changes underpinning BBB leakage [118].

There are novel MRI methods in development that use endogenous contrast which may improve sensitivity. For example, DW-pCASL employs diffusion weighting to distinguish labelled blood in the microvasculature from that in brain tissue to measure water exchange [108]. WEPCAST also employs an ASL approach using velocity encoding to isolate venous signal [109]. However, these approaches are hypothesis-based and their translation to humans would be greatly facilitated by first demonstrating that they provide reliable measures of BBB function in preclinical models.

MR Spectroscopy to Assess Metabolites

Magnetic resonance spectroscopy (MRS) determines tissue metabolite levels in vivo and would provide a promising approach to explore SVD and neurodegenerative disease progression [14, 119–122]. However, MRS has not been applied extensively in human SVD or preclinical models.

There are some practical limitations. For example, for sampling homogeneous tissue, single voxel spectroscopy (SVS) in mice requires typical volumes ca. 0.008 cm^3 [123] (0.4% of brain volume) relative to 4 cm^3 (0.03%) in humans [124] and positioning the sample volume requires structural imaging. Multi-voxel MR spectroscopic imaging (MRSI) [125] increases brain coverage and can examine metabolite distribution, although with longer acquisition times. It is important to control for disease burden and relative proportions of healthy/diseased tissue, particularly in advanced disease, and where atrophy reduces the amount of tissue to sample. It is important to establish the test-retest reliability on individual MRI scanners, particularly for lactate and coupled metabolites [126] before use in experiments although the reproducibility for detecting more abundant metabolites is generally good and several quantification approaches are available [124].

Surface and/or refined coil designs improve rodent MRS sensitivity [127] and higher field strengths provide better spectral resolution and distinction of metabolite peaks. Preclinical MRS allows cross-validation of metabolite concentrations using chemical methods, providing greater confidence scanning humans longitudinally.

Beyond proton MRS, carbon-13, oxygen-17, sodium-23 and phosphorus-31 MRS may be applied, though multinuclear equipment is needed. Contrast agents, notably deuterium [128] and thulium [129], can monitor metabolism, pH and temperature in vivo to assess disease progression or changes in ketogenic states.

Novel MRI Methods in Rodents and Scope for Rodent-Human Translation

PVS are small conduits that envelop penetrating cerebral arterioles/venules where CSF can exchange with interstitial fluid (ISF) [48]. As part of the glymphatic system, PVS are thought to clear brain fluid and waste, facilitated by aquaporin-4 (AQP4) water channel–mediated CSF-ISF exchange at the peri-capillary space before clearance to lymphatic vessels [34, 130, 131]. While aspects of the physiology are controversial [132, 133], CSF-ISF exchange studies provide opportunities to understand PVS in vascular and neurodegenerative diseases. PVS become enlarged and more visible in SVD and are associated with inflammation, impaired CVR, increased BBB permeability and vascular pulsatility [48]. Their small size makes them difficult to assess in humans. However, CSF delivery to PVS can be characterised in rodents using DCE-MRI and Gd injection into the cisterna magna CSF. Small volume infusion of Gd into the CSF pool during 3D MRI demonstrates spatially and temporally resolved solute transport through the brain [134] and can show altered PVS function with vascular risk factors. For example, type 2 diabetes mellitus rats exhibit slower Gd clearance, with accumulation and retention, enhanced perivascular arterial influx and increased hippocampal signal intensity [39]. Tracer transport mechanisms are highly complex, but pharmacokinetic models [135, 136] and mass transport algorithms [137, 138] help quantify influx/efflux contributions. An optimal mass transport analysis in SHRSP rats reveals reduced and slowed solute transport from CSF into the brain [139]. Though rare, opportunistic human studies show CSF solute transport into basal brain parenchyma over longer times with similar distributions [140–142].

Gd injection into the cisterna magna in humans is not a practical technique; Gd injections into the lumbar CSF and tracking through the intracranial CSF have been done rarely and only when diagnosing pathological conditions. More clinically applicable although less sensitive techniques to track PVS function include diffusion imaging, PC-MRI and ultrafast MR imaging. In rodents, T2-w diffusion techniques showed CSF in PVS preferentially moved parallel to blood flow fluctuating with cardiac pulsation, consistent with PVS-CSF movement [143] but has yet to be applied in humans. PC-MRI shows that intracranial arterial, venous and CSF pulsatility in the main cisterns, correlate with WMH burden in SVD [144–146], depends on directional flow and is less suited to understanding water mobility within the brain. Magnetic resonance encephalography (MREG) is an emerging high temporal resolution sequence, which is thought to reveal spatial-temporal patterns driven by different cardiac, respiratory and vasomotor forces highlighting that cerebral water movement is directional and cyclic with several drivers [147]. Recent work with APQ4-deficient mice suggests multi-echo ASL may provide insight into clearance mechanisms [148]. Such methods may reveal new insights into SVD, particularly large calibre vessel pulsatility effects on spatiotemporal water movement characteristics, although preclinical validation remains key.

Discussion

Major advances have occurred in understanding human SVD, thanks to modern MRI methods; however, large gaps in knowledge remain which could be addressed through a range of SVD models and capitalising on multiple forms of clinically relevant image contrasts available with MRI. We demonstrate the need for greater transferability and reproducibility of preclinical-clinical MRI findings. There are numerous relevant rodent models for SVD. However, as yet, the imaging approaches do not appear to be taking full advantage of the knowledge derived from characterising human disease and thus limit the translational potential of rodent models in SVD. Further studies to ascertain key features of SVD and disease progression would help focus preclinical rodent models on the most salient features, whether structural or dynamic measures (e.g. WMH and PVS burden, cerebrovascular reactivity, BBB leakage etc). Many of the imaging techniques commonly used clinically have already been applied to various rodent models, including structural MR and techniques to investigate BBB integrity. However, several structural sequences are necessary in human MRI to capture the features properly and this approach could improve the yield of preclinical MRI. Closer matching of clinical to preclinical imaging protocols may aid comparisons of data and provide a fuller picture of differences in SVD disease progression and manifestations.

Only limited use has been made of ex vivo MRI and histology in studying SVD to date, though potentially relevant protocols exist for several relevant features. Greater use of these techniques may help determine which cellular mechanisms are at work, while improving understanding of the genesis and evolution of lesions and other imaging features, such as WMH and CMBs. Availability of human tissue, particularly from intermediate disease states, remains an obstacle; however, many questions can be explored with greater use of animal histology, in vivo and PM-MRI.

For dynamic imaging methods in rodents, determining the optimal anaesthetic regimen and the effect on derived imaging metrics is a significant challenge, but would help improve comparability between preclinical and hence clinical studies. Rodent models allow direct in vivo validation which would significantly advance understanding of underlying disease mechanisms, and emerging imaging methods, including synthetic MRI [149], with the potential to quantify disease-related tissue properties in vivo. Using comparable processing and

analysis methods in preclinical and clinical imaging will greatly increase translational potential [113]. Application of similar image analysis methods to animal and human studies is entirely feasible, would avoid repeating the same errors, improve translation and is encouraged [22, 54, 115].

Preclinical models have also enabled advances in understanding of microvascular dysfunction underlying SVD and methods to measure paravascular transport. While the initial approaches, based on relatively invasive techniques, are not applicable in routine clinical studies, it has stimulated interest in alternative imaging methods for humans which show some promise.

Imaging of SVD is key to advancing understanding of disease pathophysiology and aiding the development of novel treatments. There is immense untapped potential for clinical research to inform preclinical work and vice versa. To maximise the benefits of research into SVD, there is a need for greater engagement and active collaborations between clinical and preclinical researchers to develop research programmes taking full account of the latest advances in both domains.

Funding This work was supported by the Fondation Leducq (ref no. 16 CVD 05); the EU Horizon2020, PHC-03-15, project No 666881, 'SVDs@Target'; the MRC UK Dementia Research Institute at the University of Edinburgh and the British Heart Foundation Centre for Research Excellence Edinburgh. MS received a travel grant from the SINAPSE PECRE scheme. The work of BVZ is supported by the National Institutes of Health (NIH) grant nos. R01AG023084, R01NS090904, R01NS034467, R01AG039452, 1R01NS100459 and 5P01AG052350, and in addition to the Alzheimer's Association strategic 509279 grant and the Foundation Leducq Transatlantic Network of Excellence for the Study of Perivascular Spaces in Small Vessel Disease reference no. 16 CVD 05.

Data Availability Supplementary material including the search strategy is available on the Translational Stroke Research website.

Compliance with Ethical Standards

Conflict of Interest The authors declare that they have no conflict of interest.

Ethical Approval All procedures performed in studies involving human participants were in accordance with the ethical standards of the institutional and/or national research committee and with the 1964 Helsinki declaration and its later amendments or comparable ethical standards.

Informed Consent Informed consent was obtained from all individual participants included in the study.

References

1. Wardlaw JM, Smith C, Dichgans M. Small vessel disease: mechanisms and clinical implications. Lancet Neurol. 2019;18(7):684–96.
2. Hachinski V, Einhäupl K, Ganten D, Alladi S, Brayne C, Stephan BCM, et al. Preventing dementia by preventing stroke: the Berlin Manifesto. Alzheimers Dement. 2019;15(7):961–84.
3. Wardlaw JM, Smith EE, Biessels GJ, Cordonnier C, Fazekas F, Frayne R, et al. Neuroimaging standards for research into small vessel disease and its contribution to ageing and neurodegeneration. Lancet Neurol. 2013;12(8):822–38.
4. Thrippleton MJ, Backes WH, Sourbron S, et al. Quantifying BBB leakage in small vessel disease: review and consensus recommendations. Alzheimers Dement. 2019;15(6):840–858.
5. Van Everdingen KJ, Van der Grond J, Kappelle LJ, et al. Diffusion-weighted magnetic resonance imaging in acute stroke. Stroke. 1998;29(9):1783–90.
6. Guio FD, Jouvent E, Biessels GJ, et al. Reproducibility and variability of quantitative magnetic resonance imaging markers in cerebral small vessel disease. J Cereb Blood Flow Metab. 2016;36(8):1319–37.
7. Shi Y, Thrippleton MJ, Makin SD, Marshall I, Geerlings MI, de Craen AJM, et al. Cerebral blood flow in small vessel disease: a systematic review and meta-analysis. J Cereb Blood Flow Metab. 2016;36(10):1653–67.
8. Blair GW, Doubal FN, Thrippleton MJ, Marshall I, Wardlaw JM. Magnetic resonance imaging for assessment of cerebrovascular reactivity in cerebral small vessel disease: a systematic review. J Cereb Blood Flow Metab. 2016;36(5):833–41.
9. Farrall AJ, Wardlaw JM. Blood-brain barrier: ageing and microvascular disease – systematic review and meta-analysis. Neurobiol Aging. 2009;30(3):337–52.
10. Wardlaw JM, Makin SJ, Hernández MCV, et al. Blood-brain barrier failure as a core mechanism in cerebral small vessel disease and dementia: evidence from a cohort study. Alzheimers Dement. 2017;13(6):634–43.
11. Montagne A, Barnes SR, Sweeney MD, Halliday MR, Sagare AP, Zhao Z, et al. Blood-brain barrier breakdown in the aging human hippocampus. Neuron. 2015;85(2):296–302.
12. Nation DA, Sweeney MD, Montagne A, Sagare AP, D'Orazio LM, Pachicano M, et al. Blood-brain barrier breakdown is an early biomarker of human cognitive dysfunction. Nat Med. 2019;25(2):270–6.
13. Auer DP, Schirmer T, Heidenreich JO, Herzog J, Putz B, Dichgans M. Altered white and gray matter metabolism in CADASIL: a proton MR spectroscopy and 1H-MRSI study. Neurology. 2001;56(5):635–42.
14. Nitkunan A, Charlton RA, McIntyre DJO, et al. Diffusion tensor imaging and MR spectroscopy in hypertension and presumed cerebral small vessel disease. Magn Reson Med. 2008;59(3):528–34.
15. Bailey EL, McCulloch J, Sudlow C, Wardlaw JM. Potential animal models of lacunar stroke. Stroke. 2009;40(6):e451–8.

16. Hainsworth AH, Markus HS. Do in vivo experimental models reflect human cerebral small vessel disease? A systematic review. J Cereb Blood Flow Metab. 2008;28(12):1877–91.
17. Hainsworth AH, Allan SM, Boltze J, Cunningham C, Farris C, Head E, et al. Translational models for vascular cognitive impairment: a review including larger species. BMC Med. 2017;15(1): 16.
18. Bailey EL, Smith C, Sudlow CLM, Wardlaw JM. Is the spontaneously hypertensive stroke prone rat a pertinent model of sub cortical ischemic stroke? A systematic review. Int J Stroke. 2011;6(5):434–44.
19. Montagne A, Nikolakopoulou AM, Zhao Z, Sagare AP, Si G, Lazic D, et al. Pericyte degeneration causes white matter dysfunction in the mouse central nervous system. Nat Med. 2018;24(3): 326–37.
20. Yang Y, Kimura-Ohba S, Thompson J, Rosenberg GA. Rodent models of vascular cognitive impairment. Transl Stroke Res. 2016;7(5):407-14.
21. Zhou M, Mao L, Wang Y, Wang Q, Yang Z, Li S, Li L. Morphologic changes of cerebral veins in hypertensive rats: venous collagenosis is associated with hypertension. J Stroke Cerebrovasc Dis. 2015; 24(3):530-6.
22. Holland PR, Searcy JL, Salvadores N, Scullion G, Chen G, Lawson G, et al. Gliovascular disruption and cognitive deficits in a mouse model with features of small vessel disease. J Cereb Blood Flow Metab. 2015;35(6):1005–14.
23. Liu Q, Radwanski R, Babadjouni R, Patel A, Hodis DM, Baumbacher P, et al. Experimental chronic cerebral hypoperfusion results in decreased pericyte coverage and increased blood-brain barrier permeability in the corpus callosum. J Cereb Blood Flow Metab. 2019;39(2):240–50.
24. Joutel A, Monet-Leprêtre M, Gosele C, Baron-Menguy C, Hammes A, Schmidt S, et al. Cerebrovascular dysfunction and microcirculation rarefaction precede white matter lesions in a mouse genetic model of cerebral ischemic small vessel disease. J Clin Invest. 2010;120(2):433–45.
25. Trouillet A, Lorach H, Dubus E, el Mathari B, Ivkovic I, Dégardin J, et al. Col4a1 mutation generates vascular abnormalities correlated with neuronal damage in a mouse model of HANAC syndrome. Neurobiol Dis. 2017;100:52–61.
26. McColl BW, Carswell HV, McCulloch J, et al. Extension of cerebral hypoperfusion and ischaemic pathology beyond MCA territory after intraluminal filament occlusion in C57Bl/6J mice. Brain Res. 2004;997(1):15–23.
27. Oliff HS, Coyle P, Weber E. Rat strain and vendor differences in collateral anastomoses. J Cereb Blood Flow Metab. 1997;17(5): 571–6.
28. Uludağ K, Blinder P. Linking brain vascular physiology to hemodynamic response in ultra-high field MRI. NeuroImage. 2018;168:279–95.
29. Durukan A, Tatlisumak T. Acute ischemic stroke: overview of major experimental rodent models, pathophysiology, and therapy of focal cerebral ischemia. Pharmacol Biochem Behav. 2007;87(1):179–97.
30. Paasonen J, Salo RA, Shatillo A, Forsberg MM, Närväinen J, Huttunen JK, et al. Comparison of seven different anesthesia protocols for nicotine pharmacologic magnetic resonance imaging in rat. Eur Neuropsychopharmacol. 2016;26(3):518–31.
31. Percie du Sert N, Alfieri A, Allan SM, et al. The IMPROVE guidelines (ischaemia models: procedural refinements of in vivo experiments). J Cereb Blood Flow Metab. 2017;37(11):3488–517.
32. Benveniste H, Lee H, Ding F, Sun Q, al-Bizri E, Makaryus R, et al. Anesthesia with dexmedetomidine and low-dose isoflurane increases solute transport via the glymphatic pathway in rat brain when compared with high-dose isoflurane. Anesthesiology. 2017;127(6):976–88.
33. Pedder H, Vesterinen HM, Macleod MR, Wardlaw JM. Systematic review and meta-analysis of interventions tested in animal models of lacunar stroke. Stroke. 2014;45(2):563–70.
34. Iliff JJ, Wang M, Liao Y, et al. A paravascular pathway facilitates CSF flow through the brain parenchyma and the clearance of interstitial solutes, including amyloid β. Sci Transl Med. 2012;4(147):147ra111.
35. Peng W, Achariyar TM, Li B, Liao Y, Mestre H, Hitomi E, et al. Suppression of glymphatic fluid transport in a mouse model of Alzheimer's disease. Neurobiol Dis. 2016;93:215–25.
36. Mestre H, Kostrikov S, Mehta R, et al. Perivascular spaces, glymphatic dysfunction, and small vessel disease. Clin Sci. 2017;131(17):2257–74.
37. Benveniste H, Heerdt PM, Fontes M, et al. Glymphatic system function in relation to anesthesia and sleep states. Anesth Analg. 2019;128(4):747–58.
38. Mestre H, Tithof J, Du T, et al. Flow of cerebrospinal fluid is driven by arterial pulsations and is reduced in hypertension. Nat Commun. 2018;9:4878.
39. Jiang Q, Zhang L, Ding G, Davoodi-Bojd E, Li Q, Li L, et al. Impairment of the glymphatic system after diabetes. J Cereb Blood Flow Metab. 2017;37(4):1326–37.
40. Hooijmans CR, Tillema A, Leenaars M, Ritskes-Hoitinga M. Enhancing search efficiency by means of a search filter for finding all studies on animal experimentation in PubMed. Lab Anim. 2010;44(3):170–5.
41. Rosenberg GA, Wallin A, Wardlaw JM, Markus HS, Montaner J, Wolfson L, et al. Consensus statement for diagnosis of subcortical small vessel disease. J Cereb Blood Flow Metab. 2016;36(1):6–25.
42. Kincses ZT, Király A, Veréb D, Vécsei L. Structural magnetic resonance imaging markers of Alzheimer's disease and its retranslation to rodent models. J Alzheimers Dis. 2015;47(2):277–90.
43. Beckmann N. Probing cerebrovascular alterations in Alzheimer's disease using MRI: from transgenic models to patients. Curr Med Imaging Rev. 2011;7(1):51–61.
44. Braakman N, Buchem VMA, Schliebs R, et al. Recent advances in visualizing Alzheimer's plaques by magnetic resonance imaging. Curr Med Imaging Rev. 2009;5(1):2–9.
45. Delatour B, Epelbaum S, Petiet A, Dhenain M. In vivo imaging biomarkers in mouse models of Alzheimer's disease: are we lost in translation or breaking through? Int J Alzheimers Dis. 2010;2010: 604853.
46. Pan WJ, Billings JCW, Grooms JK, Shakil S, Keilholz SD. Considerations for resting state functional MRI and functional connectivity studies in rodents. Front Neurosci. 2015; 9:269.
47. Muir KW, Macrae IM. Neuroimaging as a selection tool and endpoint in clinical and pre-clinical trials. Transl Stroke Res. 2016;7(5):368–77.
48. Wardlaw JM, Benveniste H, Nedergaard M, et al. Perivascular spaces in the brain: anatomy, physiology and pathology. Nat Rev Neurol. 2020;16(3):137–53.
49. Keene CD, Darvas M, Kraemer B, et al. Neuropathological assessment and validation of mouse models for Alzheimer's disease: applying NIA-AA guidelines. Pathobiol Aging Age Relat Dis. 2016;6:32397.
50. Holland PR, Bastin ME, Jansen MA, et al. MRI is a sensitive marker of subtle white matter pathology in hypoperfused mice. Neurobiol Aging. 2011;32(12):2325.e1–6.
51. Chaumeil MM, Valette J, Baligand C, Brouillet E, Hantraye P, Bloch G, et al. pH as a biomarker of neurodegeneration in Huntington's disease: a translational rodent-human MRS study. J Cereb Blood Flow Metab. 2012;32(5):771–9.

52. Meadowcroft MD, Connor JR, Smith MB, Yang QX. MRI and histological analysis of beta-amyloid plaques in both human Alzheimer's disease and APP/PS1 transgenic mice. J Magn Reson Imaging. 2009;29(5):997–1007.
53. Wang H, Jiang Q, Shen Y, et al. The capability of detecting small vessels beyond the conventional MRI sensitivity using iron-based contrast agent enhanced susceptibility weighted imaging. NMR Biomed. 2020;33(5):e4256.
54. Sawiak SJ, Wood NI, Williams GB, Morton AJ, Carpenter TA. Voxel-based morphometry with templates and validation in a mouse model of Huntington's disease. Magn Reson Imaging. 2013;31(9):1522–31.
55. Li Y, Shen Q, Huang S, Li W, Muir ER, Long JA, et al. Cerebral angiography, blood flow and vascular reactivity in progressive hypertension. Neuroimage. 2015;111:329–37.
56. Fazekas F, Chawluk JB, Alavi A, Hurtig HI, Zimmerman RA. MR signal abnormalities at 1.5 T in Alzheimer's dementia and normal aging. Am J Roentgenol. 1987;149(2):351–6.
57. Cordonnier C, Potter GM, Jackson CA, Doubal F, Keir S, Sudlow CLM, et al. Improving interrater agreement about brain microbleeds: development of the Brain Observer MicroBleed Scale (BOMBS). Stroke. 2009;40(1):94–9.
58. Benveniste H, Einstein G, Kim KR, Hulette C, Johnson GA. Detection of neuritic plaques in Alzheimer's disease by magnetic resonance microscopy. Proc Natl Acad Sci U S A. 1999;96(24):14079–84.
59. Deshmane A, Gulani V, Griswold MA, Seiberlich N. Parallel MR imaging. J Magn Reson Imaging. 2012;36(1):55–72.
60. Kayvanrad M, Lin A, Joshi R, Chiu J, Peters T. Diagnostic quality assessment of compressed sensing accelerated magnetic resonance neuroimaging. J Magn Reson Imaging. 2016;44(2):433–44.
61. Kaiser D, Weise G, Möller K, Scheibe J, Pösel C, Baasch S, et al. Spontaneous white matter damage, cognitive decline and neuroinflammation in middle-aged hypertensive rats: an animal model of early-stage cerebral small vessel disease. Acta Neuropathol Commun. 2014;2:169.
62. Humphreys CA, Jansen MA, Muñoz Maniega S, González-Castro V, Pernet C, Deary IJ, Salman RAS, Wardlaw JM, Smith C. A protocol for precise comparisons of small vessel disease lesions between ex vivo magnetic resonance imaging and histopathology. Int J Stroke. 2019;14(3):310–320.
63. Black SE, Gao F, Bilbao J. Understanding white matter disease: imaging-pathological correlations in vascular cognitive impairment. Stroke. 2009;40(3 Suppl):S48–52.
64. Pfefferbaum A, Sullivan EV, Adalsteinsson E, Garrick T, Harper C. Postmortem MR imaging of formalin-fixed human brain. Neuroimage. 2004;21(4):1585–95.
65. Dawe RJ, Bennett DA, Schneider JA, Vasireddi SK, Arfanakis K. Postmortem MRI of human brain hemispheres: T2 relaxation times during formaldehyde fixation. Magn Reson Med. 2009;61(4):810–8.
66. Shepherd TM, Thelwall PE, Stanisz GJ, Blackband SJ. Aldehyde fixative solutions alter the water relaxation and diffusion properties of nervous tissue. Magn Reson Med. 2009;62(1):26–34.
67. van Duijn S, Nabuurs RJA, van Rooden S, Maat-Schieman MLC, van Duinen SG, van Buchem MA, et al. MRI artifacts in human brain tissue after prolonged formalin storage. Magn Reson Med. 2011;65(6):1750–8.
68. de Reuck J, Auger F, Cordonnier C, et al Comparison of 7.0-T T_2*-magnetic resonance imaging of cerebral bleeds in postmortem brain sections of Alzheimer patients with their neuropathological correlates. Cerebrovasc Dis. 2011;31(5):511–7.
69. McFadden WC, Walsh H, Richter F, et al. Perfusion fixation in brain banking: a systematic review. Acta Neuropathol Commun. 2019;7(1):146.
70. Gibson LM, Chappell FM, Summers D, Collie DA, Sellar R, Best J, et al. Post-mortem magnetic resonance imaging in patients with suspected prion disease: pathological confirmation, sensitivity, specificity and observer reliability. A national registry. PLoS One. 2018;13(8):e0201434.
71. van Veluw SJ, Charidimou A, van der Kouwe AJ, et al. Microbleed and microinfarct detection in amyloid angiopathy: a high-resolution MRI-histopathology study. Brain. 2016;139(12):3151–62.
72. McAleese KE, Alafuzoff I, Charidimou A, et al. Post-mortem assessment in vascular dementia: advances and aspirations. BMC Med. 2016;14(1):129.
73. Young VG, Halliday GM, Kril JJ. Neuropathologic correlates of white matter hyperintensities. Neurology. 2008;71(11):804–11.
74. Murray ME, Vemuri P, Preboske GM, Murphy MC, Schweitzer KJ, Parisi JE, et al. A quantitative postmortem MRI design sensitive to white matter hyperintensity differences and their relationship with underlying pathology. J Neuropathol Exp Neurol. 2012;71(12):1113–22.
75. Keith J, Gao F, Noor R, Kiss A, Balasubramaniam G, Au K, Rogaeva, Masellis M, Black SE. Collagenosis of the deep medullary veins: an underrecognized pathologic correlate of white matter hyperintensities and periventricular infarction? J Neuropathol Exp Neurol. 2017;76(4):299–312.
76. McAleese KE, Firbank M, Hunter D, et al. Magnetic resonance imaging of fixed post mortem brains reliably reflects subcortical vascular pathology of frontal, parietal and occipital white matter. Neuropathol Appl Neurobiol. 2013;39(5):485–97.
77. Hernández MCV, Piper RJ, Bastin ME, Royle NA, Maniega SM, Aribisala BS, et al. Morphologic, distributional, volumetric, and intensity characterization of periventricular hyperintensities. Am J Neuroradiol. 2014;35(1):55–62.
78. Sun SW, Neil JJ, Liang HF, He YY, Schmidt RE, Hsu CY, et al. Formalin fixation alters water diffusion coefficient magnitude but not anisotropy in infarcted brain. Magn Reson Med. 2005;53(6):1447–51.
79. Shereen A, Nemkul N, Yang D, Adhami F, Dunn RS, Hazen ML, et al. Ex vivo diffusion tensor imaging and neuropathological correlation in a murine model of hypoxia-ischemia-induced thrombotic stroke. J Cereb Blood Flow Metab. 2011;31(4):1155–69.
80. van Veluw SJ, Shih AY, Smith EE, et al. Detection, risk factors, and functional consequences of cerebral microinfarcts. Lancet Neurol. 2017;16(9):730–40.
81. Smith EE, Schneider JA, Wardlaw JM, Greenberg SM. Cerebral microinfarcts: the invisible lesions. Lancet Neurol. 2012;11(3):272–82.
82. Van Veluw SJ, Zwanenburg JJM, Rozemuller AJM, et al. The spectrum of MR detectable cortical microinfarcts: a classification study with 7-tesla postmortem MRI and histopathology. J Cereb Blood Flow Metab. 2015;35(4):676–83.
83. Cordonnier C, Al-Shahi Salman R, Wardlaw J. Spontaneous brain microbleeds: systematic review, subgroup analyses and standards for study design and reporting. Brain. 2007;130(8):1988–2003.
84. de Reuck JL, Deramecourt V, Auger F, Durieux N, Cordonnier C, Devos D, et al. The significance of cortical cerebellar microbleeds and microinfarcts in neurodegenerative and cerebrovascular diseases. Cerebrovasc Dis. 2015;39(2):138–43.
85. Shoamanesh A, Kwok CS, Benavente O. Cerebral microbleeds: histopathological correlation of neuroimaging. Cerebrovasc Dis. 2011;32(6):528–34.
86. Gomori JM, Grossman RI. Mechanisms responsible for the MR appearance and evolution of intracranial hemorrhage. Radiographics. 1988;8(3):427–40.
87. Fazekas F, Kleinert R, Roob G, Kleinert G, Kapeller P, Schmidt R, et al. Histopathologic analysis of foci of signal loss on gradient-

echo T2*-weighted MR images in patients with spontaneous intracerebral hemorrhage: evidence of microangiopathy-related microbleeds. Am J Neuroradiol. 1999;20(4):637–42.
88. Reuter B, Venus A, Heiler P, et al. Development of cerebral microbleeds in the APP23-transgenic mouse model of cerebral amyloid angiopathy - a 9.4 tesla MRI study. Front Aging Neurosci. 2016;8:170.
89. Luo F, Rustay NR, Seifert T, Roesner B, Hradil V, Hillen H, et al. Magnetic resonance imaging detection and time course of cerebral microhemorrhages during passive immunotherapy in living amyloid precursor protein transgenic mice. J Pharmacol Exp Ther. 2010;335(3):580–8.
90. Beckmann N, Doelemeyer A, Zurbruegg S, Bigot K, Theil D, Frieauff W, et al. Longitudinal noninvasive magnetic resonance imaging of brain microhemorrhages in BACE inhibitor-treated APP transgenic mice. Neurobiol Aging. 2016;45:50–60.
91. Adams LC, Bressem K, Böker SM, Bender YNY, Nörenberg D, Hamm B, et al. Diagnostic performance of susceptibility-weighted magnetic resonance imaging for the detection of calcifications: a systematic review and meta-analysis. Sci Rep. 2017;7(1):15506.
92. Klohs J, Deistung A, Schweser F, Grandjean J, Dominietto M, Waschkies C, et al. Detection of cerebral microbleeds with quantitative susceptibility mapping in the ArcAbeta mouse model of cerebral amyloidosis. J Cereb Blood Flow Metab. 2011;31(12):2282–92.
93. Fantini S, Sassaroli A, Tgavalekos KT, Kornbluth J. Cerebral blood flow and autoregulation: current measurement techniques and prospects for noninvasive optical methods. Neurophotonics. 2016;3(3):031411.
94. Alsop DC, Detre JA, Golay X, Günther M, Hendrikse J, Hernandez-Garcia L, et al. Recommended implementation of arterial spin-labeled perfusion MRI for clinical applications: a consensus of the ISMRM perfusion study group and the European consortium for ASL in dementia. Magn Reson Med. 2015;73(1):102–16.
95. Kim T, Richard Jennings J, Kim SG. Regional cerebral blood flow and arterial blood volume and their reactivity to hypercapnia in hypertensive and normotensive rats. J Cereb Blood Flow Metab. 2014;34(3):408–14.
96. Leoni RF, Paiva FF, Henning EC, Nascimento GC, Tannús A, de Araujo DB, et al. Magnetic resonance imaging quantification of regional cerebral blood flow and cerebrovascular reactivity to carbon dioxide in normotensive and hypertensive rats. Neuroimage. 2011;58(1):75–81.
97. Tancredi FB, Hoge RD. Comparison of cerebral vascular reactivity measures obtained using breath-holding and CO2 inhalation. J Cereb Blood Flow Metab. 2013;33(7):1066–74.
98. Peppel P, Anton F. Responses of rat medullary dorsal horn neurons following intranasal noxious chemical stimulation: effects of stimulus intensity, duration, and interstimulus interval. J Neurophysiol. 1993;70(6):2260–75.
99. Thrippleton MJ, Shi Y, Blair G, Hamilton I, Waiter G, Schwarzbauer C, et al. Cerebrovascular reactivity measurement in cerebral small vessel disease: rationale and reproducibility of a protocol for MRI acquisition and image processing. Int J Stroke. 2018;13(2):195–206.
100. Kisler K, Nelson AR, Rege SV, Ramanathan A, Wang Y, Ahuja A, Lazic D, Tsai PS, Zhao Z, Zhou Y, Boas DA, Sakadžić, Zlokovic BV. Pericyte degeneration leads to neurovascular uncoupling and limits oxygen supply to brain. Nat Neurosci. 2017;20(3):406–416.
101. Zhao Z, Nelson AR, Betsholtz C, Zlokovic BV. Establishment and dysfunction of the blood-brain barrier. Cell. 2015;163(5):1064–78.
102. Montagne A, Nation DA, Pa J, Sweeney MD, Toga AW, Zlokovic BV. Brain imaging of neurovascular dysfunction in Alzheimer's disease. Acta Neuropathol. 2016;131(5):687–707.
103. Zlokovic BV, Griffin JH. Cytoprotective protein C pathways and implications for stroke and neurological disorders. Trends Neurosci. 2011;34(4):198–209.
104. Drouin-Ouellet J, Sawiak SJ, Cisbani G, Lagacé M, Kuan WL, Saint-Pierre M, et al. Cerebrovascular and blood-brain barrier impairments in Huntington's disease: potential implications for its pathophysiology. Ann Neurol. 2015;78(2):160–77.
105. Sweeney MD, Sagare AP, Zlokovic BV. Blood-brain barrier breakdown in Alzheimer disease and other neurodegenerative disorders. Nat Rev Neurol. 2018;14(3):133–50.
106. van De Haar HJ, Burgmans S, Jansen JFA, et al. Blood-brain barrier leakage in patients with early Alzheimer disease. Radiology. 2016;281(2):527–35.
107. Montagne A, Nation DA, Sagare AP, et al. APOE4 leads to blood-brain barrier dysfunction predicting cognitive decline. Nature. 2020;581(7806):71–6.
108. Palomares JA, Tummala S, Wang DJJ, Park B, Woo MA, Kang DW, et al. Water exchange across the blood-brain barrier in obstructive sleep apnea: an MRI diffusion-weighted pseudo-continuous arterial spin labeling study. J Neuroimaging. 2015;25(6):900–5.
109. Lin Z, Li Y, Su P, Mao D, Wei Z, Pillai JJ, et al. Non-contrast MR imaging of blood-brain barrier permeability to water. Magn Reson Med. 2018;80(4):1507–20.
110. Absinta M, Ha SK, Nair G, Sati P, Luciano NJ, Palisoc M, et al. Human and nonhuman primate meninges harbor lymphatic vessels that can be visualized noninvasively by MRI. Elife. 2017;6:e29738.
111. O'Connor JPB, Tofts PS, Miles KA, Parkes LM, Thompson G, Jackson A. Dynamic contrast-enhanced imaging techniques: CT and MRI. Br J Radiol. 2011;84(Spec Iss 2):S112–20.
112. Heye AK, Thrippleton MJ, Armitage PA, Valdés Hernández MC, Makin SD, Glatz A, et al. Tracer kinetic modelling for DCE-MRI quantification of subtle blood–brain barrier permeability. NeuroImage. 2016;125:446–55.
113. Barnes SR, Ng TSC, Montagne A, Law M, Zlokovic BV, Jacobs RE. Optimal acquisition and modeling parameters for accurate assessment of low Ktrans blood-brain barrier permeability using dynamic contrast-enhanced MRI. Magn Reson Med. 2016;75(5):1967–77.
114. Barnes SL, Whisenant JG, Loveless ME, Yankeelov TE. Practical dynamic contrast enhanced MRI in small animal models of cancer: data acquisition, data analysis, and interpretation. Pharmaceutics. 2012;4(3):442–78.
115. Barnes SR, Ng TSC, Santa-Maria N, Montagne A, Zlokovic BV, Jacobs RE. ROCKETSHIP: a flexible and modular software tool for the planning, processing and analysis of dynamic MRI studies. BMC Med Imaging. 2015;15:19.
116. Wilson MH, Davagnanam I, Holland G, Dattani RS, Tamm A, Hirani SP, et al. Cerebral venous system and anatomical predisposition to high-altitude headache. Ann Neurol. 2013;73(3):381–9.
117. Geurts LJ, Bhogal AA, Siero JCW, Luijten PR, Biessels GJ, Zwanenburg JJM. Vascular reactivity in small cerebral perforating arteries with 7 T phase contrast MRI – a proof of concept study. NeuroImage. 2018;172:470–7.
118. Bell RD, Winkler EA, Singh I, Sagare AP, Deane R, Wu Z, et al. Apolipoprotein E controls cerebrovascular integrity via cyclophilin A. Nature. 2012;485(7399):512–6.
119. Dedeoglu A, Choi JK, Cormier K, Kowall NW, Jenkins BG. Magnetic resonance spectroscopic analysis of Alzheimer's disease mouse brain that express mutant human APP shows altered neurochemical profile. Brain Res. 2004;1012(1-2):60–5.

120. Zhu M, Akimana C, Wang E, Ng CK. 1H-MRS quantitation of age-dependent taurine changes in mouse brain. Mol Imaging Biol. 2019;21(5):812–817.
121. Marjanska M, Curran GL, Wengenack TM, Henry PG, Bliss RL, Poduslo JF, et al. Monitoring disease progression in transgenic mouse models of Alzheimer's disease with proton magnetic resonance spectroscopy. Proc Natl Acad Sci U S A. 2005;102(33): 11906–10.
122. Kantarci K. Proton MRS in mild cognitive impairment. J Magn Reson Imaging. 2013;37(4):770–7.
123. Lee MR, Denic A, Hinton DJ, Mishra PK, Choi DS, Pirko I, et al. Preclinical 1H-MRS neurochemical profiling in neurological and psychiatric disorders. Bioanalysis. 2012;4(14):1787–804.
124. Wilson M, Andronesi O, Barker PB, Bartha R, Bizzi A, Bolan PJ, et al. Methodological consensus on clinical proton MRS of the brain: review and recommendations. Magn Reson Med. 2019;82(2):527–50.
125. Posse S, Otazo R, Dager SR, Alger J. MR spectroscopic imaging: principles and recent advances. J Magn Reson Imaging. 2013;37(6):1301–25.
126. Ramadan S, Lin A, Stanwell P. Glutamate and glutamine: a review of in vivo MRS in the human brain. NMR Biomed. 2013;26(12): 1630–46.
127. Tkáč I. Methodology of MRS in Animal Models: Technical Challenges and Solutions. In: Öz G. (eds) Magnetic Resonance Spectroscopy of Degenerative Brain Diseases. Contemporary Clinical Neuroscience. Cham: Springer; 2016. p. 13-30.
128. Feyter DHM, Behar KL, Corbin ZA, et al. Deuterium metabolic imaging (DMI) for MRI-based 3D mapping of metabolism in vivo. Sci Adv. 2018;4(8):eaat7314.
129. Coman D, Trubel HK, Rycyna RE, Hyder F. Brain temperature and pH measured by 1H chemical shift imaging of a thulium agent. NMR Biomed. 2009;22(2):229–39.
130. Rennels ML, Blaumanis OR, Grady PA. Rapid solute transport throughout the brain via paravascular fluid pathways. Adv Neurol. 1990;52:431–9.
131. Tarasoff-Conway JM, Carare RO, Osorio RS, Glodzik L, Butler T, Fieremans E, et al. Clearance systems in the brain-implications for Alzheimer disease. Nat Rev Neurol. 2015;11(8):457–70.
132. Abbott NJ, Pizzo ME, Preston JE, Janigro D, Thorne RG. The role of brain barriers in fluid movement in the CNS: is there a 'glymphatic' system? Acta Neuropathol. 2018;135(3):387–407.
133. Smith AJ, Yao X, Dix JA, Jin BJ, Verkman AS. Test of the 'glymphatic' hypothesis demonstrates diffusive and aquaporin-4-independent solute transport in rodent brain parenchyma. Elife. 2017;6:e27679.
134. Iliff JJ, Lee H, Yu M, Feng T, Logan J, Nedergaard M, et al. Brain-wide pathway for waste clearance captured by contrast-enhanced MRI. J Clin Invest. 2013;123(3):1299–309.
135. Davoodi-Bojd E, Ding G, Zhang L, Li Q, Li L, Chopp M, et al. Modeling glymphatic system of the brain using MRI. NeuroImage. 2019;188:616–27.
136. Lee H, Xie L, Yu M, Kang H, Feng T, Deane R, et al. The effect of body posture on brain glymphatic transport. J Neurosci. 2015;35: 11034–44.
137. Ratner V, Gao Y, Lee H, Elkin R, Nedergaard M, Benveniste H, et al. Cerebrospinal and interstitial fluid transport via the glymphatic pathway modeled by optimal mass transport. Neuroimage. 2017;152:530–7.
138. Elkin R, Nadeem S, Haber E, Steklova K, Lee H, Benveniste H, Tannenbaum A. GlymphVIS: visualizing glymphatic transport pathways using regularized optimal transport. In: Frangi A, Schnabel J, Davatzikos C, Alberola-López C, Fichtinger G, editors. Medical Image Computing and Computer Assisted Intervention – MICCAI 2018. MICCAI 2018. Lecture Notes in Computer Science, vol 11070. Cham: Springer; 2018. p. 844–853.
139. Koundal S, Elkin R, Nadeem S, et al. Optimal mass transport with Lagrangian workflow reveals advective and diffusion driven solute transport in the glymphatic system. Sci Rep. 2020;10(1):1990.
140. Ringstad G, Vatnehol SAS, Eide PK. Glymphatic MRI in idiopathic normal pressure hydrocephalus. Brain. 2017;140(10): 2691–705.
141. Ringstad G, Valnes LM, Dale AM, , Pripp AH, Vatnehol SAS, Emblem KE, Mardal KA, Eide PK. Brain-wide glymphatic enhancement and clearance in humans assessed with MRI. JCI Insight. 2018;3(13):e121537.
142. Watts R, Steinklein JM, Waldman L, Zhou X, Filippi CG. Measuring glymphatic flow in man using quantitative contrast-enhanced MRI. Am J Neuroradiol. 2019;40(4):648–651.
143. Harrison IF, Siow B, Akilo AB, Evans PG, Ismail O, Ohene Y, et al. Non-invasive imaging of CSF-mediated brain clearance pathways via assessment of perivascular fluid movement with diffusion tensor MRI. Elife. 2018;7:e34028.
144. Shi Y, Thrippleton MJ, Blair GW, et al. Small vessel disease is associated with altered cerebrovascular pulsatility but not resting cerebral blood flow. J Cereb Blood Flow Metab. 2020;40(1):85–99.
145. Makedonov I, Black SE, MacIntosh BJ. BOLD fMRI in the white matter as a marker of aging and small vessel disease. PLoS One. 2013;8(7):e67652.
146. Lau KK, Pego P, Mazzucco S, Li L, Howard DPJ, Küker W, et al. Age and sex-specific associations of carotid pulsatility with small vessel disease burden in transient ischemic attack and ischemic stroke. Int J Stroke. 2018;13(8):832–9.
147. Kiviniemi V, Wang X, Korhonen V, Keinänen T, Tuovinen T, Autio J, et al. Ultra-fast magnetic resonance encephalography of physiological brain activity–glymphatic pulsation mechanisms? J Cereb Blood Flow Metab. 2016;36(6):1033–45.
148. Ohene Y, Harrison IF, Nahavandi P, Ismail O, Bird EV, Ottersen OP, et al. Non-invasive MRI of brain clearance pathways using multiple echo time arterial spin labelling: an aquaporin-4 study. NeuroImage. 2019;188:515–23.
149. Tanenbaum LN, Tsiouris AJ, Johnson AN, Naidich TP, DeLano MC, Melhem ER, et al. Synthetic MRI for clinical neuroimaging: results of the magnetic resonance image compilation (MAGiC) prospective, multicenter, multireader trial. Am J Neuroradiol. 2017;38(6):1103–10.